Physica A 185 (1992) 129–145
North-Holland

PHYSICA A

Equivalence between the Abelian sandpile model and the $q \to 0$ limit of the Potts model

S.N. Majumdar and Deepak Dhar

Theoretical Physics Group, Tata Institute of Fundamental Research, Homi Bhabha Road, Bombay 400005, India

We establish an equivalence between the undirected Abelian sandpile model and the $q \to 0$ limit of the q-state Potts model. The equivalence is valid for arbitrary finite graphs. Two-dimensional Abelian sandpile models, thus, correspond to a conformal field theory with central charge $c = -2$. The equivalence also gives a Monte Carlo algorithm to generate random spanning trees. We study the growth process of the spread of fire under the burning algorithm in the background of a random recurrent configuration of the Abelian sandpile model. The average number of sites burnt upto time t varies at t^a. In two dimensions our numerically determined value of a agrees with the theoretical prediction $a = 8/5$. We relate this exponent to the conventional exponents characterizing the distributions of avalanche sizes.

1. Introduction

In recent years the concept of self-organized criticality (SOC) has attracted much attention [1–5]. It has been found useful in the description of such diverse systems as earthquakes [6–8], forest fires [4], relaxation phenomena in magnets [9, 10] and coagulation [11]. Bak et al. in their pioneer papers [1, 2] introduced the concept through the example of sandpiles, which have been extensively studied [12–16] as paradigms of self-organized critical systems. Sandpile-like lattice models have been used to describe fracture [17], neural networks [18] and hydrogen bonding in liquid water [19]. Of special interest are the so-called Abelian sandpile models [20] (ASMs) as they provide a nontrivial, analytically tractable example of SOC. In an earlier paper [20], we have shown that if the toppling condition at a lattice site depends only on the height of sandpile at that site and not on heights at other sites, operators corresponding to sandgrain addition at different sites commute. This Abelian property was used to analytically determine the steady state of the model, and also some response functions and the spectrum of relaxation times in the critical state.

While there has been much interest in the study of ASMs [21–26], so far only some of the critical exponents of interest have been determined analytical-

ly. All the critical exponents in d-dimensions are known exactly only for ASMs with a preferred direction, which are in the same universality class as the voter model [27]. For undirected ASMs, exponents characterizing the distribution of avalanche sizes have been determined analytically only for the Bethe lattice ($d = \infty$) [28] and in the mean field theory [29–31]. It is known [20] that the two point correlation function measuring the expected number of topplings at a point at distance r from the point where sand is added varies as r^{2-d} for large r in d dimensions. Also, the correlation between heights of sandpile at two sites separated by r varies as r^{-2d} [32]. Only numerical estimates are available so far for the exponents characterizing the distribution of avalanches by their duration, linear extent, number of topplings, etc.

This paper is organized as follows. In section 2, we establish an equivalence between the steady state of the ASM defined on arbitrary graph G and the spanning trees problem on a related graph G′, obtained by connecting one extra site to G. The number of stable configurations that occur with nonzero probability in the steady state of the ASM equals the number of spanning trees on G′. We establish a one to one correspondence between allowed configurations (those which occur with nonzero probability in the steady state) of ASM on G and the spanning trees on G′. This then gives us an unbiased algorithm to generate spanning trees. In section 3, using the known relation between spanning trees and the q-state Potts model, we get an equivalence between the ASM and the $q \to 0$ limit of the q-state Potts model. Our knowledge of critical exponents of the latter in two dimensions from conformal field theory thus helps us determine exactly one more critical exponent for the ASM in two dimensions. In section 4, we study numerically a growth model where the fire spreads under the burning algorithm in the background of a random recurrent configuration of ASM and in particular show that the dynamical exponent z of the growth model is equal to the fractal dimension of the backbone of random spanning trees. In section 5, we establish some scaling relations between the different exponents of avalanche distributions of ASM and relate them to z.

2. Equivalence of ASM to spanning trees problem

We start by recalling the definition of the general ASM on a set of N sites labelled $1, 2, \ldots, N$. At each site i, the height of the sandpile is given by an integer z_i. Addition of sand corresponds to increasing the height of the pile by unity at a site chosen at random. If the height at any site i exceeds a critical value z_{ic}, that site topples and all the variables z_j ($j = 1, \ldots, N$) are updated according to the rule

$$z_j \to z_j - \Delta_{ij} , \qquad \text{for all } j ,$$

where Δ_{ij} is an integer matrix satisfying

$$\Delta_{ii} > 0 , \quad \Delta_{ij} \leq 0 \quad \text{and} \quad \sum_j \Delta_{ij} \geq 0 .$$

In this paper, we restrict our attention to undirected graphs so that the matrix Δ is symmetric,

$$\Delta_{ij} = \Delta_{ji} , \qquad \text{for all } i \text{ and } j .$$

We can represent the toppling rules by a graph G′ containing $N+1$ sites, labelled $0, 1, 2, \ldots, N$. The graph has multiple links allowed, and the number of links between sites i and j (i and j both nonzero) equal $|\Delta_{ij}|$. For all $i \neq 0$, we connect site i to site 0 using $(\Sigma_{j=1}^{N} \Delta_{ij})$ links. The site 0 represents the sink, so that on a single toppling at site i, the number of sandgrains lost from the system (which is $\Sigma_{j=1}^{N} \Delta_{ij}$) equals the number of sandgrains transferred from i to 0.

We have earlier introduced a burning algorithm to distinguish between stable configurations of the sandpile that occur with nonzero probability in the steady state, and those that do not [20]. In this algorithm, it does not matter in which order the sites are burnt. It is, however, useful to introduce the concept of time of burning. This is done quite simply as follows: At time $t = 0$, all sites of the graph G′ are unburnt, except 0 which is burnt. At any time, an unburnt site i is called "burnable" iff z_i strictly exceeds the number of edges connecting i to other unburnt sites. A burnable site at time t becomes burnt at time $t+1$, and stays burnt at all subsequent times.

We note that the growth of fire is deterministic for a given configuration of heights of the sandpile. The stochastic character comes from the randomness in this background configuration as in case of invasion percolation [33]. We have shown earlier that a configuration occurs with a nonzero probability in the steady state if and only if eventually all the sites of the graph get burnt under this algorithm.

Take an arbitrary site i. Let τ_i be the time step at which this is burnable. Then we say that $\tau_i + 1$ is the burning time of the site i. Then from our burning rules it follows that site i must have at least one neighbour (site connected by an edge) whose burning time is τ_i. Let r_i be the number of such neighbours. Let us write

$$\xi_i = \sum_j{}' (-\Delta_{ij}) ,$$

where the primed summation is over all unburnt neighbours j of i at time τ_i. Then, since site i is burnable at time τ_i, we have $z_i > \xi_i$. Also, since the site was not burnable at time $\tau_i - 1$, we must also have

$$z_i \leq \xi_i + K ,$$

where K is the number of distinct edges connecting i to its r_i neighbours which were burnt at time τ_i. We say that fire reaches the site i by one of these K bonds. If $K = 1$, there is only one possibility and there is no problem. If $K > 1$, we shall select the bond by which the fire reaches i depending on z_i. For this purpose, we order all the edges incident on site i in some order of preference. This ordering is arbitrary, and can be chosen independently for edges incident at each site i. Then, if $z_i = \xi_i + s$, we say that fire reach site i using the sth bond from the ordered list of K bonds connecting site i to its neighbours burnt at τ_i.

Clearly, this prescription gives a unique path to the fire reaching site i, given the configuration of heights of the sandpile. The set of all bonds along which fire propagates connects 0 to the rest of the lattice. Each site i is thus connected to 0, and there are no loops. This set of edges thus forms a spanning tree on the graph G′. From our previous discussion, it is clear that there is a one to one correspondence between allowed configurations of height in the sandpile, and the spanning trees on G′.

In fig. 1, we have illustrated the one to one correspondence between spanning trees and the allowed configurations of ASM. Fig. 1a shows an allowed height configuration for an ASM on a 4×4 square lattice. Fig. 1b shows the corresponding spanning tree where the solid line denotes the boundary treated as a single site 0. At each site (except 0) there are four bonds incident. Call them N, E, S, W depending on the direction of incidence. Let us choose the ordering (same at each site) N > E > S > W. Then for the site labelled A, which burns at $t = 1$, we have $\xi_A = 2$, $K = 2$. The fire could reach A from north or from west. We then must have $3 \leq z_A \leq 4$. Since the height is

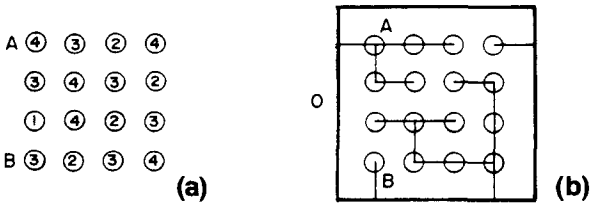

Fig. 1. (a) A typical height configuration of the ASM on a 4×4 square lattice and (b) the corresponding spanning tree. The deep solid line outside the square denotes the single sink site 0.

second of these values, we choose the bond second in preference (west) to burn A. At site B, the height variable is 3 and leads to choosing the south bond, which has higher preference compared to the west bond.

Now, determination of the number of spanning trees on a graph is a well-known problem in graph theory, and the number of trees T is given in terms of minors of the incidence matrix of the graph [34]. For the graph G′, the incidence matrix is $(N+1)\times(N+1)$ matrix $\bar{\Delta}$ obtained by adding one row and column to the matrix Δ so that

$$\sum_i \bar{\Delta}_{ij} = \sum_j \bar{\Delta}_{ji} = 0 \qquad \text{for } i = 0, \ldots, N ,$$

and

$$\bar{\Delta}_{ij} = \Delta_{ij} \qquad \text{for } i, j = 1, \ldots, N .$$

The determinant of $\bar{\Delta}$ is zero by construction, and deleting the row and column corresponding to any site (say 0), we get a matrix (in this case Δ) whose determinant equals T. We thus have

$$T = \det \Delta .$$

Since the spanning trees of G′ are in one to one correspondence with allowed configurations of the sandpile, we have still another way to derive the result that the number of allowed configurations of the ASM is given by $\det \Delta$.

We note that once an order of preference is decided for the bonds incident at all sites, we can associate a unique spanning tree with each allowed configuration of the ASM. Adding a particle and relaxing to a stable configuration gives a new allowed ASM configuration and therefore a different spanning tree on G′. We can thus study a random sequence of configurations of the ASM on G, and use the equivalence to get an unbiased Monte Carlo algorithm to generate spanning trees on a graph G′.

3. Equivalence to $q = 0$ Potts model

It is known [35] that the spanning tree problem corresponds to the q-state Potts model in the limit $q \to 0$. In our problem, assign a q-state Potts spin σ_i to each site i of G′, and consider the Potts Hamiltonian

$$H = q^{1/2} K \sum_{ij} \Delta_{ij} \delta(\sigma_i, \sigma_j) .$$

Then in the limit $q \to 0$, K fixed, the partition function of the Hamiltonian, apart from the unimportant overall normalization factor, tends to the limit

$$Z_{\text{Potts}} = q^{(N+2)/2} K^N T + \text{terms higher order in } q \, .$$

We thus have a rather unexpected equivalence between the nonequilibrium ASM and a model of equilibrium statistical mechanics. We note that the transition rates of the Markov process defined by ASM do not satisfy the detailed balance condition. In such cases, the effective Hamiltonian defined for each configuration by the logarithm of probability in the steady state usually contains long range interactions. While the enumeration of allowed configurations of ASM superficially looks like the calculation of the partition function of an ice-like model, there is an important difference: in the ice model, the constraints are local, and in a single sequential scan of the configuration, one can decide if the configuration is allowed or not. This is not so for the ASM. Similarly for spanning trees, one cannot decide if a configuration of bonds on a graph form a spanning tree in one sequential scan of the configuration.

In the $q \to 0$ limit, the Potts model is also equivalent to the resistor network problem, and its two point correlation function satisfies a linear equation. It varies as r^{2-d} for large r in d dimensions for all temperatures. Thus $q = 0$, K arbitrary is a line of critical points in the (q, K) plane. That the criticality of the model is insensitive to variations of K is a reflection of self-organized criticality in the model. Comparing with the known results of the ASM, we see that the Potts model two point correlation function corresponds to the ASM correlation function G_{ij} measuring the expected number of topplings at site i due to addition of a particle at j.

It would be interesting to identify Potts model clusters that would correspond to avalanche clusters in ASM. This seems difficult. The main problem is the absence of a natural preference order in the bijection between spanning trees and the allowed configurations of the ASM. Also the $q \to 0$ limit is somewhat formal, and it is difficult to get an intuitive understanding of the behaviour of spins in this limit.

In the rest of this paper, we shall consider only the two-dimensional ASM on the square lattice unless otherwise stated.

In the case of two dimensions, several results about the Potts model are known from Coulomb gas equivalence and conformal field theory. For example, we know that the $q \to 0$ Potts model corresponds to the conformal field theory with central charge $c = -2$. For the q-state Potts model, the energy–energy correlation function at the critical point varies as r^{-2x_T} for large separations r [35], where

$$x_T = \frac{1+y}{2-y}, \qquad y = \frac{2}{\pi}\cos^{-1}(\tfrac{1}{2}\sqrt{q}).$$

For $q = 0$, we get $x_T = 2$. Since it is known that the height–height correlation function of the ASM in d dimensions varies as r^{-2d} for large r [32], we may conclude that the height operator of the ASM corresponds, in the continuum limit, to the energy density operator of the 0-state Potts model.

It is possible to deduce that the central charge $c = -2$ for ASM using only the fact that two-dimensional ASM corresponds to a critical conformal field theory and finite size scaling. Let us consider the ASM on a finite square lattice $L \times M$. We assume periodic boundary conditions in the y-direction, and open boundary conditions in the x-direction. Then the allowed number of configurations in the SOC state of this model is

$$N = \det \Delta,$$

where Δ is the Laplacian matrix given by

$$\Delta_{r,r'} = \begin{cases} 4 & \text{if } r = r', \\ -1 & \text{if } r \text{ and } r' \text{ are nearest neighbours}, \\ 0 & \text{otherwise}. \end{cases}$$

Using the periodicity of Δ under translations in the y-direction, it is easy to show that

$$\det \Delta = \prod_{m=0}^{M-1} \frac{\lambda_+^{L+1}(2\pi m/M) - \lambda_-^{L+1}(2\pi m/M)}{\lambda_+(2\pi m/M) - \lambda_-(2\pi m/M)}, \tag{3.1}$$

where

$$\lambda_\pm(k) = 2 - \cos k \pm \sqrt{(1-\cos k)(3-\cos k)}.$$

If the logarithms of eigenvalues of the corresponding transfer matrix are μ_α ($\alpha = 1, \ldots, 4^M$), from general theory, the partition function of a system of length L along the transfer direction is of the form

$$Z_L = \sum_\alpha c_\alpha \exp(\mu_\alpha L), \tag{3.2}$$

where c_α's are some boundary condition dependent constants. Comparing eq. (3.1) with (3.2), we can write down 2^M eigenvalues of the transfer matrix for the ASM problem,

$$\mu_\alpha = \sum_{m=0}^{M-1} \epsilon_m \ln[\lambda_+(2\pi m/M)] ,$$

where $\epsilon_m = \pm 1$. Taking all $\epsilon_m = 1$ gives us the largest eigenvalue

$$\mu_1 = \sum_{m=0}^{M-1} \ln\{2 - \cos(2\pi m/M) + \sqrt{[1 - \cos(2\pi m/M)][3 - \cos(2\pi m/M)]}\} .$$

For large M, this can be simplified to give

$$\mu_1 = M \int_0^{2\pi} \frac{dk}{2\pi} \ln[\lambda_+(k)] - 2\pi/6M + \mathcal{O}(1/M^2) .$$

Since from finite size scaling theory [36], the corrections to the bulk free energy should vary as $\pi c/6M$, we see that ASM corresponds to a conformal field theory with central charge

$$c = -2 .$$

4. Numerical study of the burning process

We have studied the growth of fire in the burning algorithm in the two-dimensional ASM numerically. We considered a square lattice of size $L \times L$ with periodic boundary condition. Since for a critical steady state to exist, it should be possible for extra sand to leave the system, we puncture this torus by deleting one site (called the origin). Any sand grain falling at the origin is removed from the system.

Sandgrains are added one by one randomly. After each grain is added, we check if the resulting configuration is stable. If at any site, height of the pile exceeds 4, four grains drop from that site, one on each of the four neighbours. We relax the sandpile to a stable configuration before adding another sandgrain. This generates a sequence of stable configurations $\{C_i\}$ of the sandpile. For these configurations, we studied the growth of burnt cluster as a function of time. In practice, in order to generate a sequence of statistically uncorrelated stable configurations, we analysed only every rth configuration of the sequence $\{C_i\}$ (in our case $r = \sqrt{L}$ or more). Fig. 2 shows the growth of fire in two typical configurations. We note that the clusters are compact but quite irregular in shape. There are very few holes, and these occur only near the surface. Deep inside the burnt cluster, there can be no holes, as each hole, once generated, must shrink in size with time till it disappears.

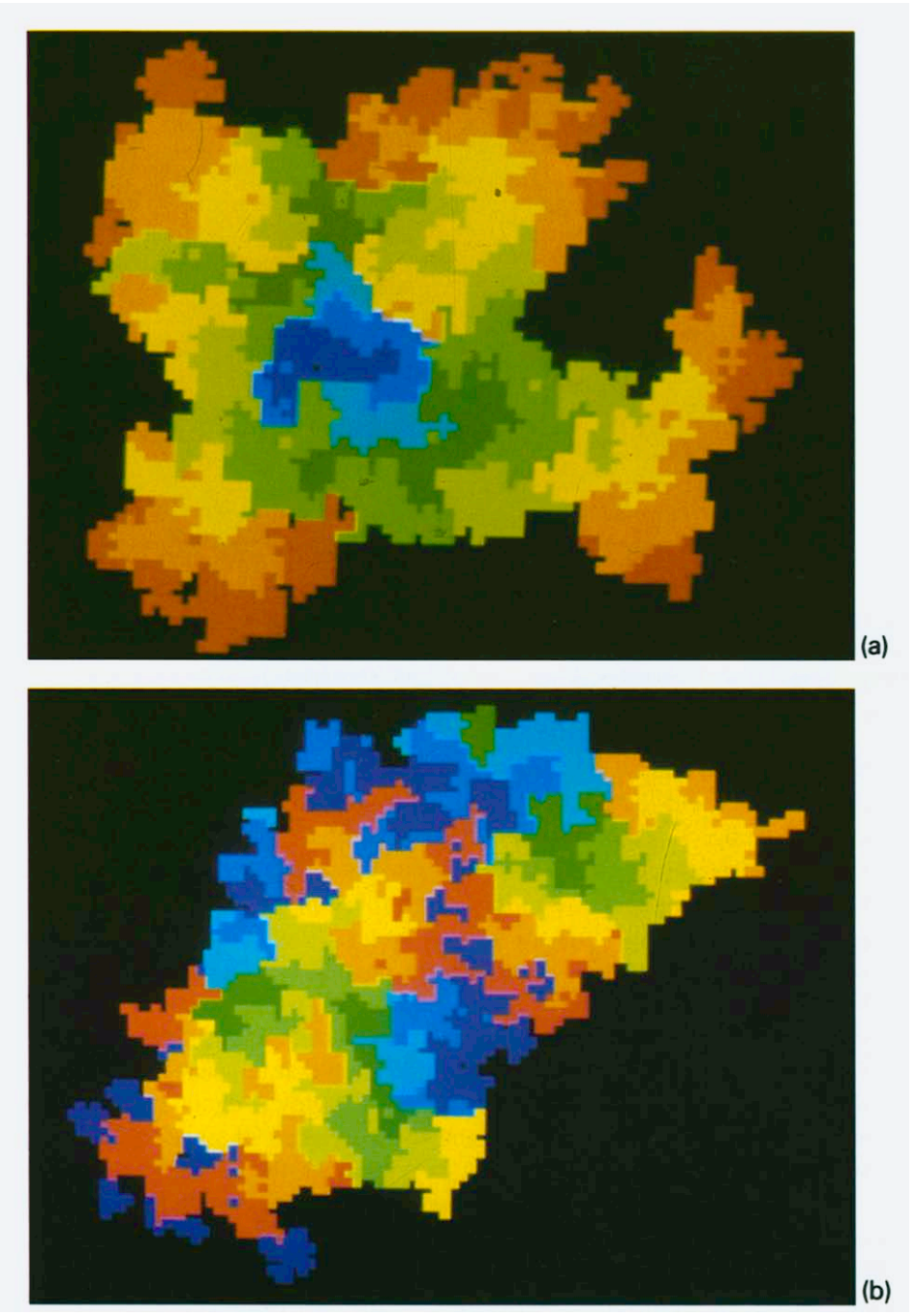

Fig. 2. Two configurations of the burnt cluster on a 121×121 lattice. The black dot, completely surrounded by deep blue region, denotes the hole at the center. The colour codes indicate the time of burning, starting with deep blue and followed by indigo, light blue, deep green, light green, yellow, orange and red. The colour changes every 4 time steps and the colour code starts repeating after red. Note the highly anisotropic growth of the cluster in (b).

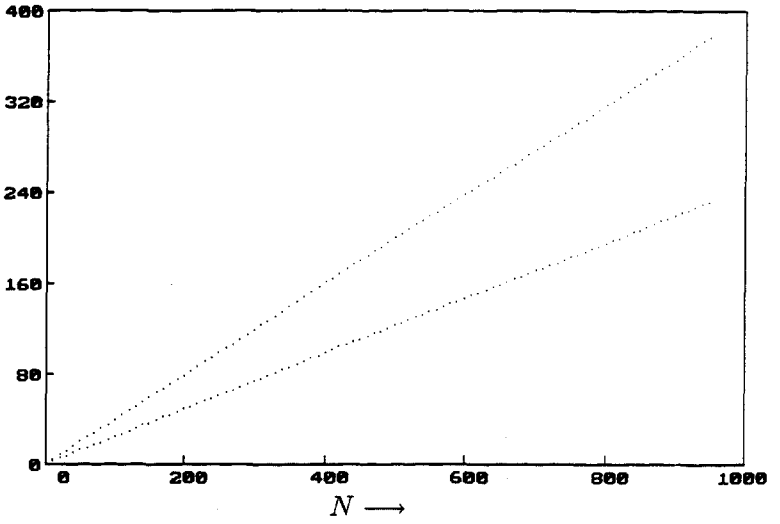

Fig. 3. The plot of I_1/N (upper curve) and I_2/N (lower curve) against N, where I_1 and I_2 are the moment of inertia of the cluster about the origin and the center of mass, respectively, and N is the number of sites in the cluster. The data is averaged over 300 configurations on a 121 × 121 lattice.

For a cluster containing N sites, we calculated the moment of inertia $I_1(N)$ about the origin, and the moment of inertia $I_2(N)$ about the center of mass of the cluster. In fig. 3, we have plotted the value of $I_1(N)/N$ and $I_2(N)/N$ as a function of N, averaged over 300 distinct clusters. These graphs show a fairly clear linear dependence of the radius of gyration on N. This is in agreement with our theoretical result that the fractal dimension of these clusters must be 2, as the clusters cannot have holes (except near the surface).

We note, however, that from our data $I_2(N)/N^2$ is approximately equal to 0.245. This value is significantly larger than the value $1/2\pi \approx 0.159$, which is the value of $I_2(N)/N^2$ for a circular disc, indicating that the cluster shape is not nearly circular. In fact, the growth of clusters is highly irregular, and in many cases, the cluster grows for a long time in one region or quadrant, with no growth at other parts of the perimeter. Note that, in the cluster shown in fig. 2b, the distance of the origin from the cluster boundary is only 3 units, while the diameter of the cluster is about 100 units.

While the actual growth of the cluster is quite erratic, some features of the growth are fairly predictable, and do not vary much from sample to sample. For example, in fig. 4, we have plotted $\langle N_t \rangle$, the total number of sites burnt upto time t versus t, for different lattice sizes. N_t is a monotonically increasing function of time t, which reaches the maximum value $N_{\max} = L^2 - 1$ at some sample dependent time t^*. At time t^*, the fire consumes the last unburnt site,

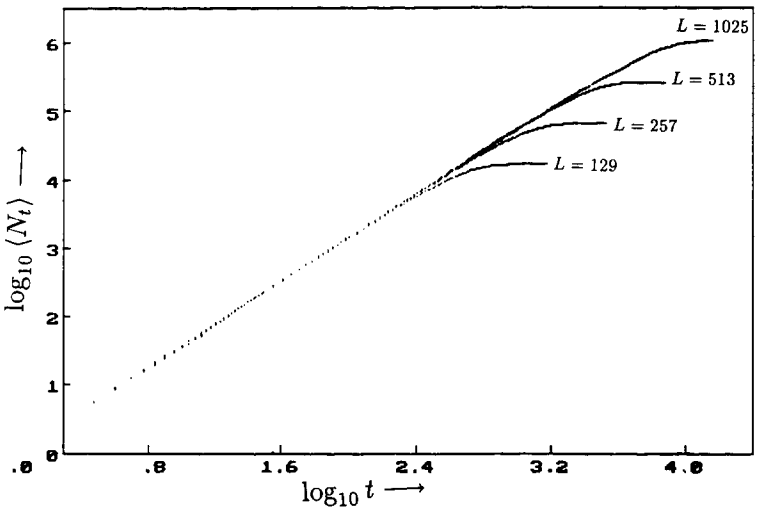

Fig. 4. The log–log plot of $\langle N \rangle_t$, the total number of sites burnt upto time t versus t for $L = 129$, 257, 513 and 1025. The corresponding number of configurations over which N_t was averaged were respectively 174 000, 29 750, 4975 and 70.

and for all $t \geq t^*$, $N_t = L^2 - 1$. For t much less than t^*, N_t increases as a power of t. The data shown in fig. 4 shows average value of N_t for lattice sizes $L = 129$, 257, 513 and 1025. The number of configurations used for averaging were 174000, 29750, 4975 and 70, respectively. We see that for $t \ll t^*$, we have

$$\langle N \rangle_t \sim t^a$$

with

$$a = 1.595 \pm 0.020$$

In fact, our data is quite consistent with the scaling form

$$\langle N \rangle_t = L^2 f(t/L^z) \tag{4.1}$$

with

$$z = 1.254 \pm 0.016 .$$

This value of exponent z agrees very well with the theoretical prediction $z = 5/4$. In fig. 5 we have plotted $\langle N \rangle_t / L^2$ as a function of t/L^z with $z = 5/4$

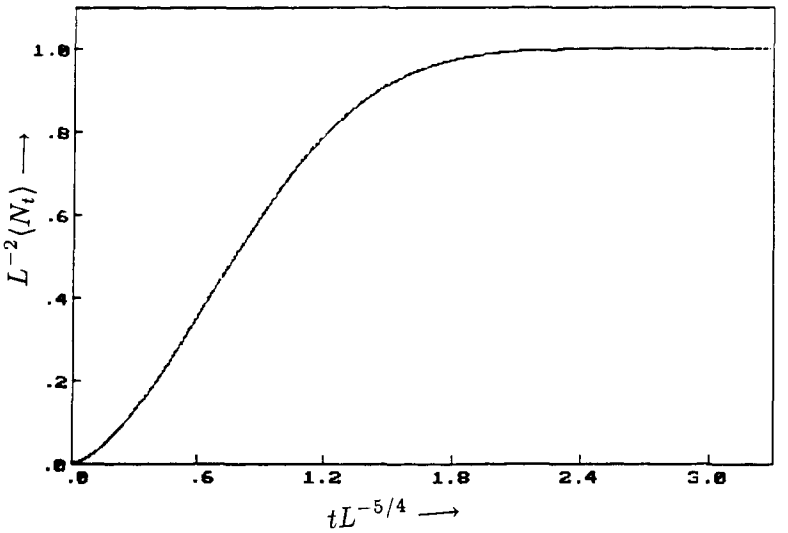

Fig. 5. The plot of $\langle N\rangle_t/L^2$ versus t/L^z for $z = 1.25$ and $L = 129$, 257 and 513. Data for different L collapse onto a single curve.

for $L = 129$, 257 and 513. The data for different L collapse nicely onto a single curve. In the spanning tree equivalence, t is just the distance along the tree (the so-called chemical distance) between the origin and the burning points on the boundary of the cluster. In the spanning tree problem, such a path may be called the backbone of the tree. But for spanning trees all the bonds in the backbone are red bonds, whose fractal dimension is known for the q-state Potts model for all q [37]. Specializing to the case $q \to 0$, these results imply that

$$t^*(L) \sim L^{5/4} .$$

Using the scaling (4.1) we then get

$$N_t \sim t^{8/5} .$$

In fig. 6 we have plotted the average number of perimeter sites of the cluster as a function of time t. We see that the average perimeter varies linearly with time, and so the fractal dimension of the perimeter of the cluster is the same as that of a typical burning path of the cluster from the origin to a point on the perimeter, and equals 5/4.

The fact that the diameter of a cluster grows slower than linearly with time,

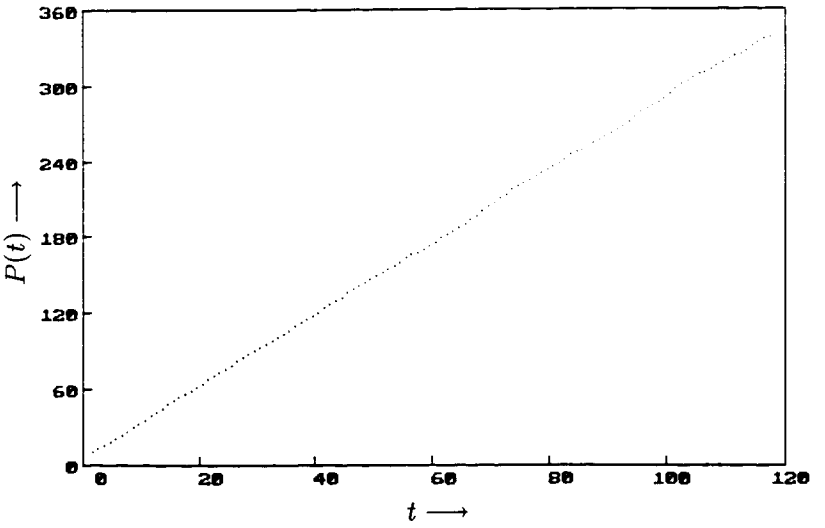

Fig. 6. The average number of perimeter sites $P(t)$ of a burning cluster at time t is plotted against t. The data is for a 121×121 lattice averaged over 100 configurations.

implies that the asymptotic velocity of the fire front tends to zero. This can be described quantitatively in terms of distribution of waiting times. We define the waiting time for burning of any site i to be $t - t'$, where t is the time step at which site i is burnt, and t' is the time step at which fire reached one of its neighbours for the first time. We define $F(\tau)$ as the probability that a randomly picked site in the cluster has a waiting time $\geqslant \tau$. In fig. 7, we plot numerically determined $F(\tau)$ versus τ. We see that this probability distribution function decays as a power law

$$F(\tau) \sim \tau^{-x}, \qquad \text{for } 1 \ll \tau \ll L^z, \tag{4.2}$$

with

$$x \approx 0.5 \pm 0.1 .$$

It is easy to understand the origin of this power law. Consider all the sites of the cluster reached upto time T. Then the sum of their waiting times so far equals $\Sigma_{t=1}^{T} P(t)$ where $P(t)$ is the perimeter at time t. But $P(t)$ increases linearly with t (fig. 4), and so the sum of waiting times increases as T^2. By definition, each of the waiting times is less then or equal to T. If we assume that the distribution of waiting times of these sites is same form as eq. (4.2)

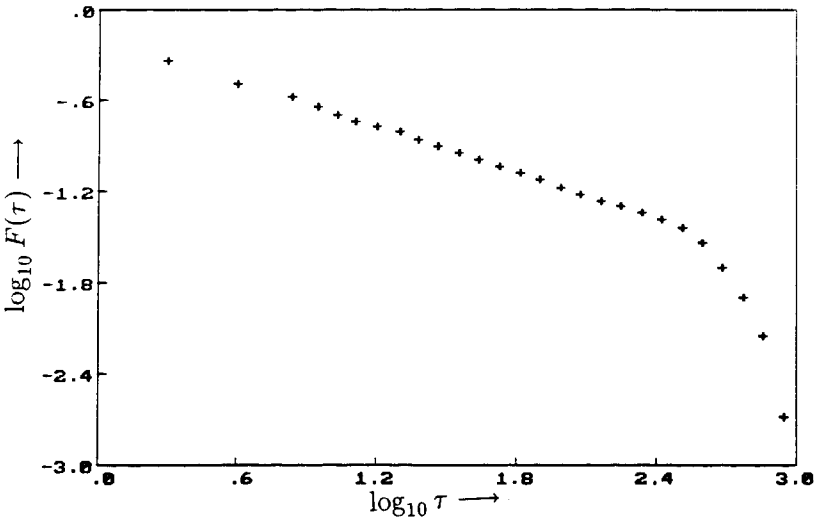

Fig. 7. The log–log plot of the cumulative waiting time distribution $F(\tau)$ versus τ, averaged over 100 configurations, for lattice size 121×121.

except an upper cutoff at $\tau = T$, we find that the mean waiting time must increase as T^{1-x}, for large T. This gives

$$x = 2/z - 1 = 3/5 ,$$

which is consistent with our numerical data.

5. Relationships between avalanche distribution exponents

There is a close connection between the avalanche clusters of the ASM and the growth clusters discussed in section 4. Given a recurrent configuration of the ASM in the one-hole geometry, suppose we "fill" the hole at 0, assign the height of the sandpile at 0 to be 5 and thus initiate an avalanche at 0. Then the cluster of distinct sites toppled at least once upto time t, is identical to the growth cluster burnt upto t for the same background configuration for all time t. The outward moving toppling front of the avalanche started at 0 proceeds exactly in the same way as that of the fire front in the corresponding growth process. It is thus possible to relate the exponents of the avalanche distributions to the dynamic exponent z of the growth process.

Let ξ denote the linear extent (diameter) of the avalanche cluster. We denote the duration of the avalanche by T. The number of distinct sites where at least

one toppling occurs will be denoted by s_d, and the total number of topplings by s. In one avalanche a particular site may topple several times, and so $s \geq s_d$. Let n_c denote the number of topplings at the site where the sandgrain causing the avalanche was added. Then ξ, T, s_d, s and n_c are stochastic variables. We introduce the exponents τ_r, τ_t, τ_d, τ_s by the relations that for large x,

$$\text{Prob}(\xi \geq x) \sim x^{-\tau_r+1}, \tag{5.1}$$

$$\text{Prob}(T \geq x) \sim x^{-\tau_t+1}, \tag{5.2}$$

$$\text{Prob}(s_d \geq x) \sim x^{-\tau_d+1}, \tag{5.3}$$

$$\text{Prob}(s \geq x) \sim x^{-\tau_s+1}. \tag{5.4}$$

The exponents τ_r, τ_t, τ_d, τ_s can be related to each other, if we make the simple scaling assumption that ξ, T, s_d and s scale as some powers of each other, i.e. if we assume all avalanches with a fixed value of one variable (say ξ), other variables T, s_d, etc. have strongly peaked conditional probability distributions. For example, from the results of previous section, T varies as ξ^z, where $z = 5/4$. This implies that

$$(\tau_t - 1) = 4(\tau_r - 1)/5. \tag{5.5}$$

Using the fact that avalanche clusters are compact, we see that $s_d \sim \xi^2$, which gives

$$(\tau_d - 1) = (\tau_r - 1)/2. \tag{5.6}$$

The calculation of τ_s requires a more elaborate argument. Since s/s_d is the average number of topplings at each toppled site, we expect that

$$s \sim s_d n_c. \tag{5.7}$$

Let us assume that n_c scales as ξ^y, where y is some exponent. Since s_d varies as ξ^2, this implies that

$$s \sim \xi^{2+y}. \tag{5.8}$$

But the exponent y can be determined in terms of τ_r again, using the result [20] that for a finite lattice of size L,

$$\langle n_c \rangle \sim \log L. \tag{5.9}$$

From eq. (5)

$$\text{Prob}(n_c \geq x) \approx \text{Prob}(\xi \geq x^{1/y}) \sim x^{-(\tau_r - 1)/y} . \tag{5.10}$$

Eq. (5.10) may be expected to hold for all $x \gg 1$, and less than some upper cutoff dependent L. This will give rise to a logarithmic dependence of L in eq. (5.9) only if

$$\text{Prob}(n_c \geq x) \sim 1/x, \qquad \text{for large } x . \tag{5.11}$$

Comparing with eq. (5.10) we see that

$$y = \tau_r - 1 . \tag{5.12}$$

Now, using Eq. (5.4) and (5.8) we get

$$(\tau_s - 1) = (\tau_r - 1)/(2 + y) = (\tau_r - 1)/(\tau_r + 1) . \tag{5.13}$$

Thus all the exponents can be expressed in terms of a single undetermined exponent, say τ_r. It would appear plausible that the exponent τ_r can also be related to some scaling exponent of the $q \to 0$ limit of the Potts model. In particular, one knows that in this limit [35], the magnetic exponent is given by

$$\beta = 1/6 .$$

We note that existing estimates of critical exponents are roughly consistent with $\tau_d \approx 7/6$, which gives $\tau_s \approx 8/7$, $\tau_t \approx 19/15$. Only Manna [15] quotes a much larger estimate of $\tau_s \approx 1.2$ and $\tau_t \approx 1.3$. Pietronero et al. [25], using a Flory-like approximation, also get $\tau_s = 8/7$. Their approximation, however, also gives $\tau_d = 1$ and $z = 4/3$, which disagrees with the scaling relation (5.6).

Theoretical determination of τ_r remains an outstanding unsolved problem.

Acknowledgements

We are thankful to Antonio Coniglio for some useful discussions, and for pointing out that in the limit $q \to 0$, the dynamical exponent z must equal the known fractal dimension of red bonds in the Potts clusters. Our earlier simulations based on smaller lattices gave a somewhat larger value of z. Larger simulations, using the better computer facilities at HLRZ, Forschungzentrum, Julich verified Coniglio's prediction. We thank Subhrangshu Manna and Rajiv

Kumar Singh for their valuable help in the numerical work. DD would like to thank Hans Herrmann for his hospitality at HLRZ, and Sidney Redner and Sergei Obukhov for some useful discussions.

References

[1] P. Bak, C. Tang and K. Wiesenfeld, Phys. Rev. Lett. 59 (1987) 381.
[2] P. Bak, C. Tang and K. Wiesenfeld, Phys. Rev. A 38 (1988) 364.
[3] L.P. Kadanoff, Physica A 163 (1990) 1.
[4] P. Bak and K. Chen, Physica D 38 (1989) 5.
[5] S.P. Obukhov, Phys. Rev. Lett. 65 (1990) 1395.
[6] J.M. Carlson and J.S. Langer, Phys. Rev. Lett. 62 (1989) 2632.
[7] A. Sornette and D. Sornette, Europhys. Lett. 9 (1989) 197.
[8] K. Chen, P. Bak and S.P. Obukhov, Phys. Rev. A 43 (1990) 625.
[9] X. Che and H. Suhl, Phys. Rev. Lett. 64 (1990) 1670; K.D. Usadel and U. Nowak, Phys. Rev. B 43 (1991) 851.
[10] D. Dhar and P.B. Thomas, preprint (1992), J. Phys. A, submitted.
[11] H. Takayasu, Phys. Rev. Lett. 63 (1989) 2563.
[12] Y.C. Zhang, Phys. Rev. Lett. 63 (1989) 470.
[13] T. Hwa and M. Kardar, Phys. Rev. Lett. 62 (1989) 1813; Physica D 38 (1989) 198.
[14] J.M. Carlson, J.T. Chayes, E.R. Grannan and G.H. Swindle, Phys. Rev. Lett. 65 (1990) 2547.
[15] S.S. Manna, Physica A 179 (1991) 249.
[16] S.C. Lee, N.Y. Liang and W.J. Tzeng, Acad. Sin. Phys. Rev. Lett. 67 (1991) 1479.
[17] H.J. Herrmann and S. Roux, Statistical Models For The Fracture Of Disordered Media (North-Holland, Amsterdam, 1990).
[18] E.N. Miranda and H.J. Herrmann, Physica A 175 (1991) 175.
[19] M. Sasai, I. Ohmine and R. Ramaswamy, J. Chem. Phys. (1992), in press.
[20] D. Dhar, Phys. Rev. Lett. 64 (1990) 1613.
[21] S.S. Manna, J. Stat. Phys. 59 (1990) 509.
[22] P. Grassberger and S.S. Manna, J. Phys. (Paris) 51 (1990) 1077.
[23] K. Wiesenfeld, J. Theiler and B. McNamara, Phys. Rev. Lett. 65 (1990) 949.
[24] S.H. Liu, T. Kaplan and L.J. Gray, Phys. Rev. A 42 (1990) 3270.
[25] L. Pietronero, P. Tartaglia and Y.C. Zhang, Physica A 173 (1991) 22.
[26] M. Creutz, Comput. Phys. 5 (1991) 198.
[27] D. Dhar and R. Ramaswamy, Phys. Rev. Lett. 63 (1989) 1659.
[28] D. Dhar and S.N. Majumdar, J. Phys. A 23 (1990) 4333.
[29] C. Tang and P. Bak, J. Stat. Phys. 51 (1988) 797.
[30] P. Alstrom, Phys. Rev. A 37 (1988) 3110.
[31] B. Gaveau and L.S. Schulman, J. Phys. A 24 (1991) L475.
[32] S.N. Majumdar and D. Dhar, J. Phys. A 24 (1991) L357.
[33] D. Wilkinson and J.F. Willemsen, J. Phys. A 16 (1983) 3365.
[34] F. Harary, Graph Theory (Addison–Wesley, Reading, MA, 1990) p. 192.
[35] F.Y. Wu, Rev. Mod. Phys. 54 (1982) 235.
[36] J.L. Cardy, Nucl. Phys. B 270 (1986) 186.
[37] A. Coniglio, Phys. Rev. Lett. 62 (1989) 3054.